Measuring Heavy and Ultra-heavy Cosmic-ray Abundances with TIGERISS

Nicholas Cannady[1,2,3] for the TIGERISS Collaboration

[1]University of Maryland, Baltimore County
[2]NASA Goddard Space Flight Center
[3]Center for Research and Exploration in Space Sciences and Technology

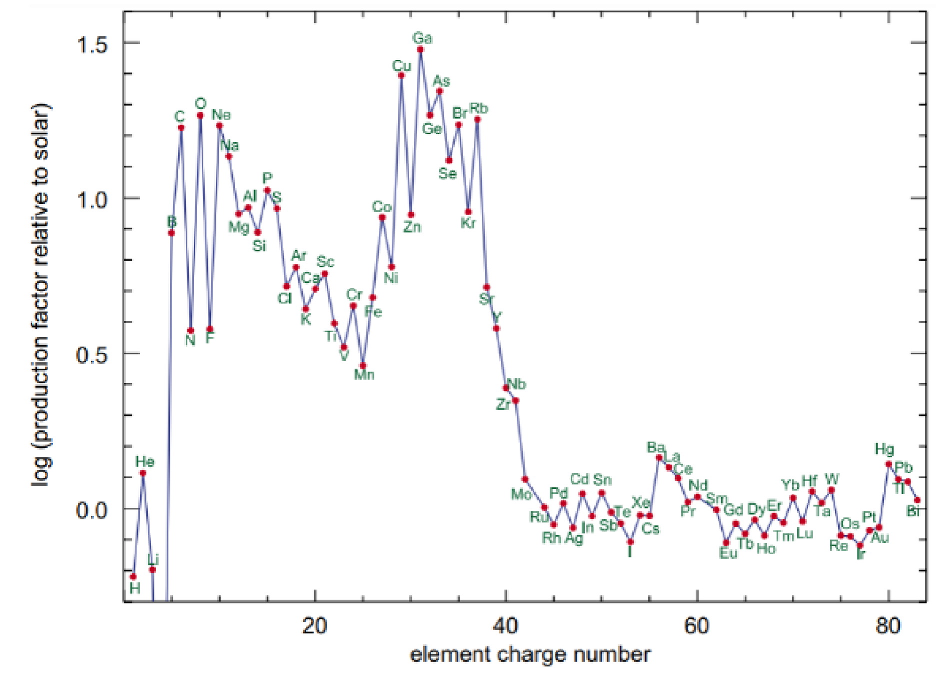

Figure 1a) **Lodders 2003** modeled core-collapse supernova yields relative to Solar System abundances

Abundances of heavy and ultra-heavy nuclei in galactic cosmic rays can constrain the source of the seed material

- Clearly differ from Solar System abundances
- Contain material present in the injection and/or the acceleration sites
- Signatures of r-process nucleosynthesis

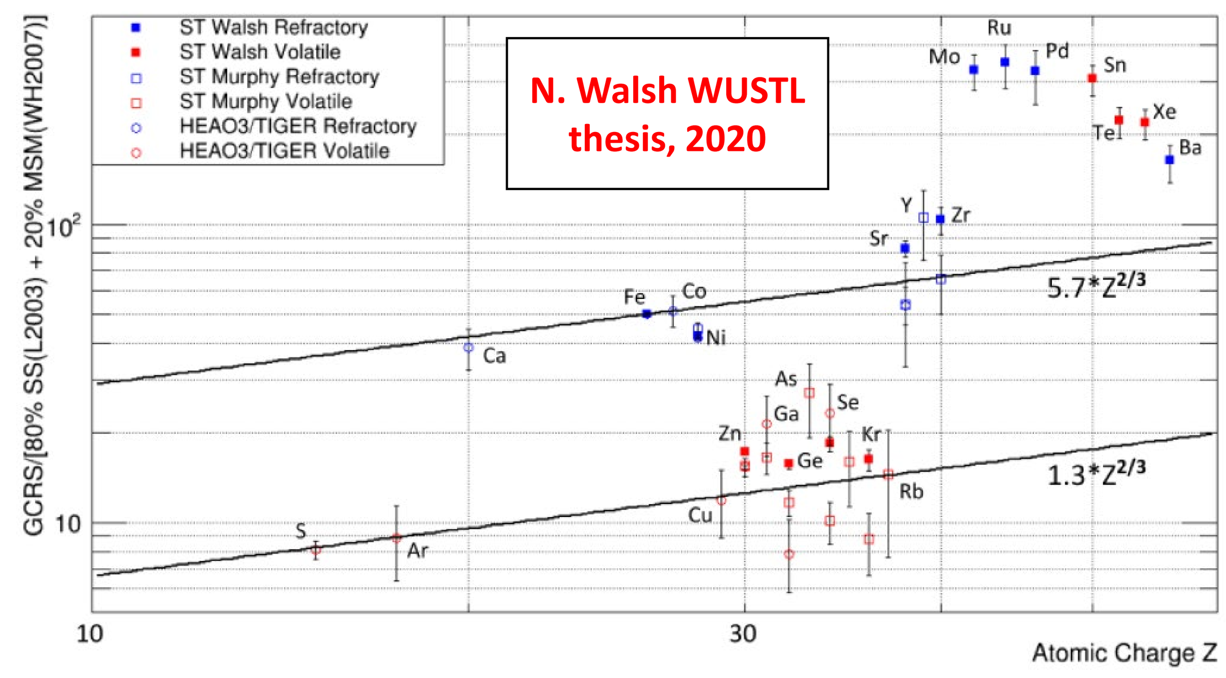

Figure 1b) Elemental abundances measured by HEAO3, TIGER, and SuperTIGER normalized to a mixture of Solar System and Massive Star Material

Observations with HEAO3 at intermediate Z and TIGER/SuperTIGER in the ultra-heavy region hint at OB association source of the GCRs (**Lingenfelter 2019**)

- Normalizing to a mixture of Solar and Massive Star Material reveals structure
- Volatile and refractory elements (from OB association temperature) separate
- Slope follows $Z^{2/3}$ dependence calculated for charge sputtering off of grains
- However: the trend appears to break down above Z = 40 (zirconium)

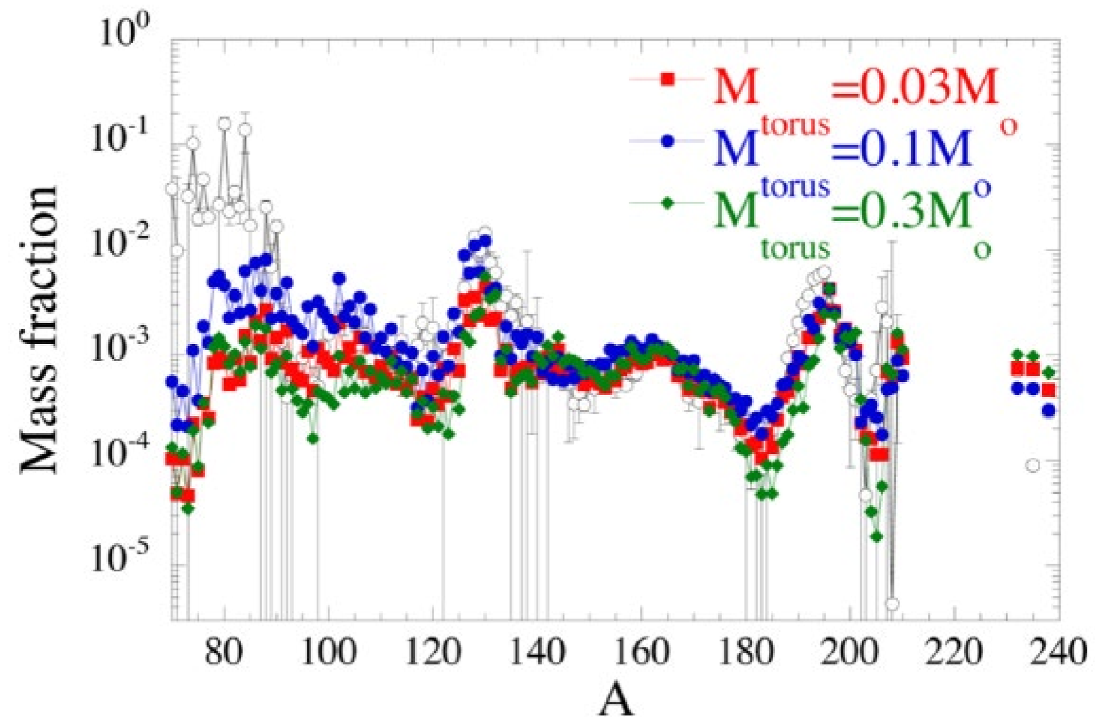

Figure 1c) **Just et al. 2015** modeled atomic yields of NS-NS and NS-BH mergers for different toroidal masses in the merger phase

GW170817/GRB 170817a demonstrated that a binary neutron star merger can create a kilonova (**Abbott et al. 2017-1, 2017-2**).

- Are BNS mergers or SNe the dominant r-process engine?
- Can a BNS merger contribution explain the change at Z = 40?

To address these questions, TIGERISS will measure abundances with single element resolution in the unprecedented range Z=5-82+

The Grand Cycle of Matter in the Galaxy (Rauch 2024)

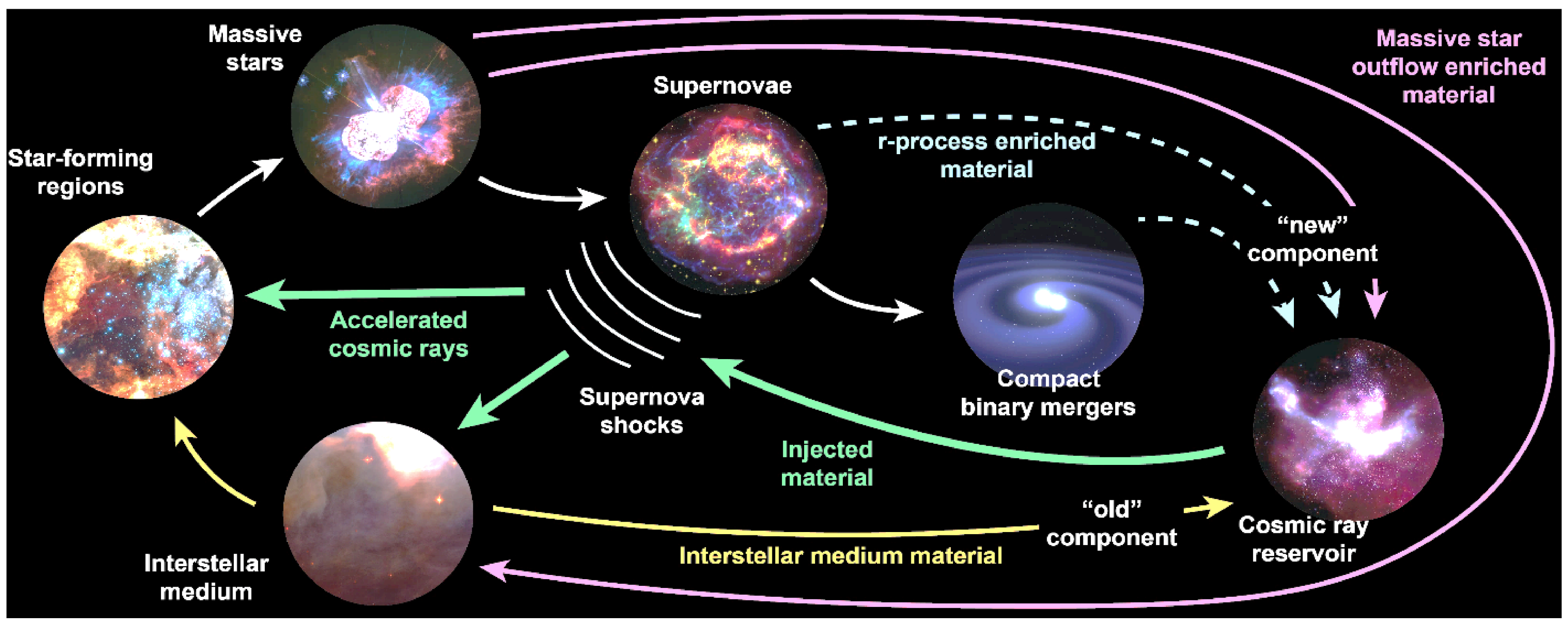

TIGERISS Detector Development

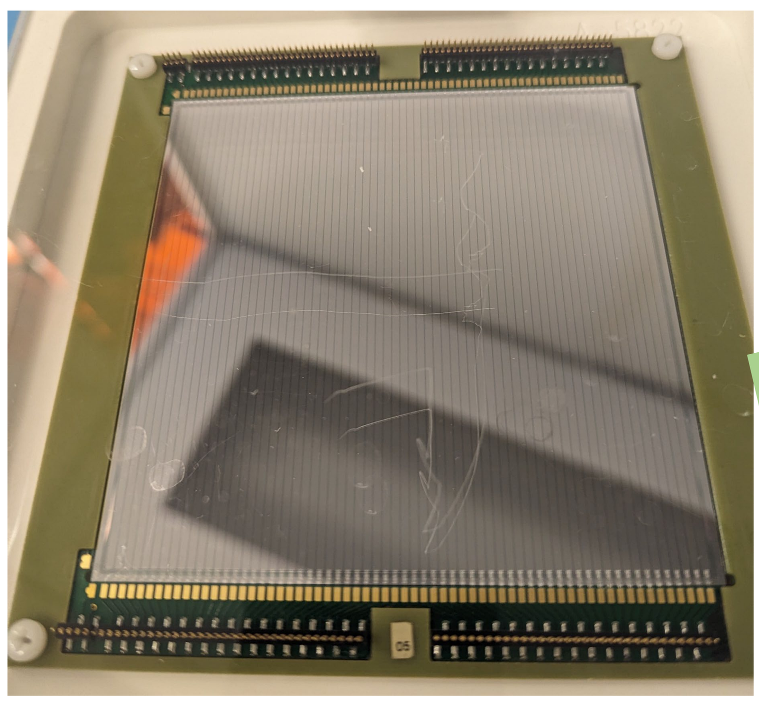

Figure 2a) Silicon strip detectors received at NASA GSFC from Micron for ADAPT. Larger strip widths will be used for the TIGERISS SSDs, which will be constructed as ladders in X and Y.

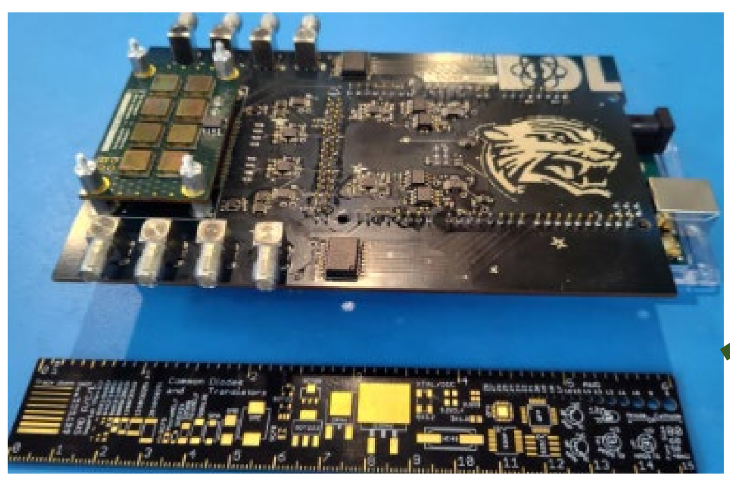

Figure 2b) Validation boards for the analog front-end design for the TIGERISS photo-detector modules. Constructed at Penn State, this large form factor unit is being tested currently to evaluate the SiPM performance.

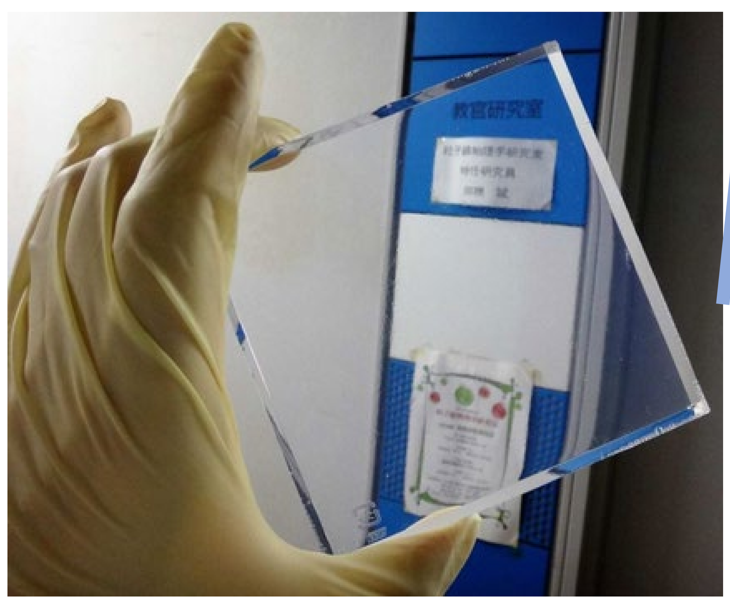

Figure 2c) A high-transparency humidity-tolerant silica aerogel tile created at Aerogel Factory in Chiba, Japan for HELIX. Sample aerogel tiles for TIGERISS are currently being procured to elevate the mechanical TRL of the array structure. The flight aerogels will follow later this summer.

The TIGERISS Instrument

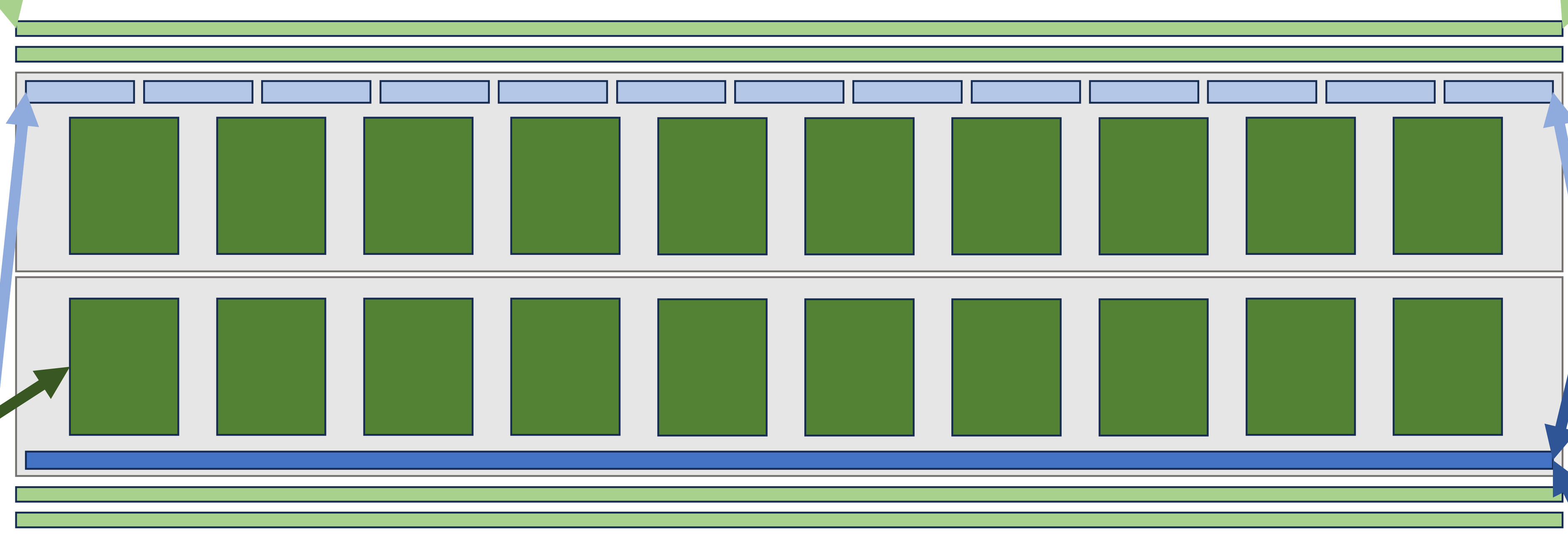

TIGERISS is to be deployed to the ISS in 2026

- Baseline location Columbus SOX
- Backup location JEM-EFU7

Four planes of single-sided **silicon strip detectors** (developed at GSFC, WUSTL)

- Micron, Hamamatsu, and FBK providing wafers
- X-Y layers alternating with 6 mm strip pitch
- Amptek A250 preamplifier-based analog FEE
- IDEAS IDE2281 (APOCAT) ASIC in digital FEE

Acrylic and aerogel **Cherenkov radiators** and boxes (developed at UMBC, GSFC)

- 5 mm thick acrylic sheet (n = 1.5)
- Aerogel Factory hydrophobic aerogels (n = 1.05)
- Aluminum box and composite support structure
- White Gore DRP lines box for effective reflection

Silicon photomultiplier based **Photo-Detector Modules** (developed at PSU, WUSTL)

- Hamamatsu S13360-6025PE
- Custom analog and digital FEE
- Active temperature compensation (a la HELIX)

Passive **thermal control system** (developed at Howard, WFF)

- Heat distribution to radiators
- Survival heaters for transition from vehicle to deployment location

Fully FPGA-based **data acquisition system** (developed at UMBC)

- No flight computer or software necessary
- Interfaces with the ISS infrastructure to receive and dispatch commands, package data, transmit data for downlink
- Zenith-looking camera support for obstruction identification in analysis

Back-end electronics and trigger system (developed at Howard, GSFC)

- BEE distributed across multiple cards, with optimal routing being studied

Power distribution unit (developed at GSFC)

- Filter and provide necessary voltages to all payload subsystems

TIGERISS Measurement Concept

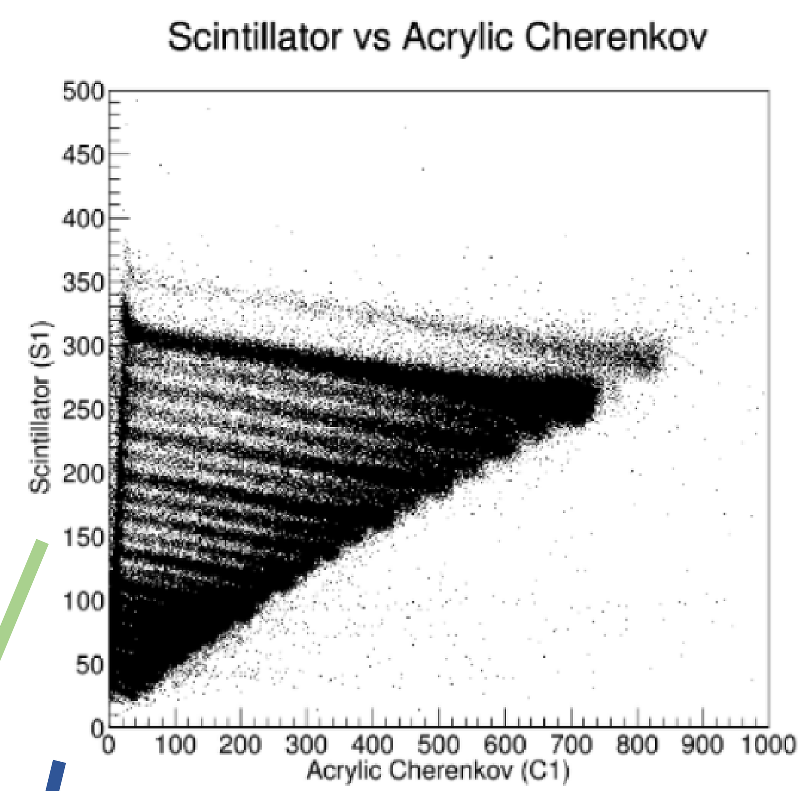

Figure 3a) Scintillator vs. acrylic Cherenkov emission for one day in the 2012 flight of SuperTIGER-2. At lower energies, only ionization measurements of the charge via the scintillators are available.

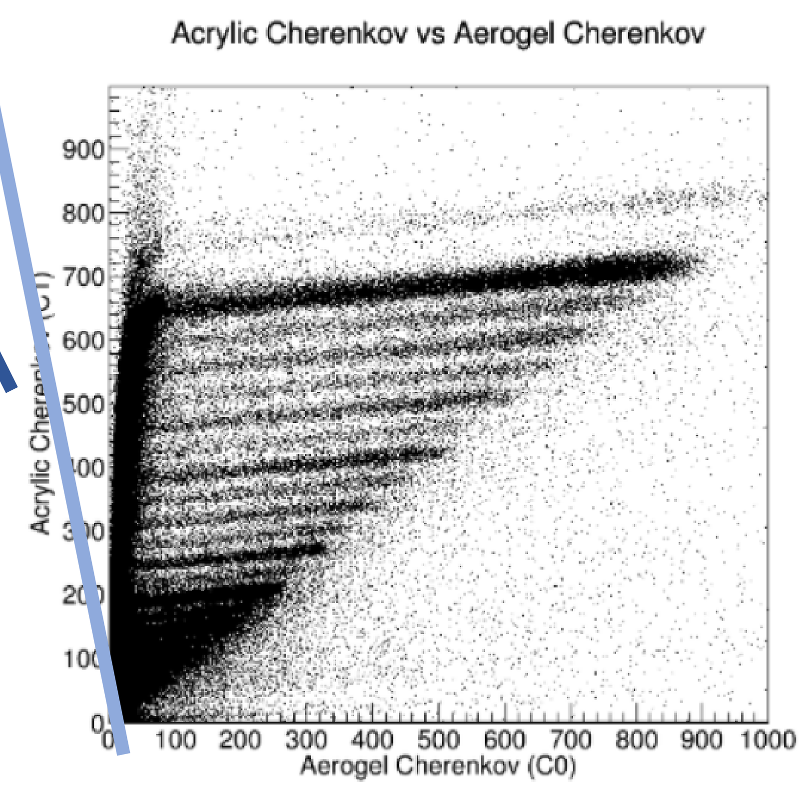

Figure 3b) Acrylic Cherenkov vs. aerogel Cherenkov for the same time period. At high velocities, signals from both radiators together can be used to further resolve the charges.

Multiple, independent measurements of the charge via ionization and Cherenkov emission decouple the charge and velocity.

Three energy (velocity) ranges:

- v < 0.67c
  Silicon detector (ionization) only
- 0.67c < v < 0.95c
  Silicon detector and acrylic Ck
- v > 0.95c
  Silicon detector, acrylic, and aerogel Ck

References

Abbott et al. 2017-1, ApJL **848** L13
Abbott et al. 2017-2, ApJL **850** L39
Just 2014, MNRAS **448** 541
Lingenfelter 2019, ApJS **245** 30
Lodders 2003, ApJ **591** 1220
Rauch et al., Instruments 2024 **8** 1
Tabata et al., NIM A **952** 161879
Walsh 2020, WUSTL PhD Thesis

Collaboration Members

R.F. Borda[6], R.G. Bose[1], D.L. Braun[1], J.H. Buckley[1], J. Calderon[4], N.W. Cannady[6], R. Caputo[2], S. Coutu[5], P. Ghosh[2], J.F. Krizmanic[2], S. Jones[4], C. Kierans[2], J.F. Krizmanic[2], W. Labrador[1], L. Lisalda[1], J.V. Martins[6], M.P. McPherson[3], E. Meyer[6], J.G. Mitchell[2], J.W. Mitchell[2], S.A.I. Mognet[5], A. Moiseev[2], G.A. de Nolfo[2], S. Nutter[4], N.E. Osborn[1], I.M. Pastrana[1], H. Salmani[3], M. Sasaki[2], G.E. Simburger[1], S. Smith[3], H.A. Tolentino[3], D. Washington[5], L.P. Williams[2]

Collaborating Institutions

[1]Washington University in St. Louis (PI Institution)
[2]NASA Goddard Space Flight Center
[3]Howard University
[4]Northern Kentucky University
[5]Penn State University
[6]University of Maryland, Baltimore County
[7]Wallops Flight Facility

Acknowledgements

The material contained in this document is based upon work supported by a National Aeronautics and Space Administration (NASA) grant or cooperative agreement. Any opinions, findings, conclusions or recommendations expressed in this material are those of the author and do not necessarily reflect the views of NASA. NASA is supported under the NASA Astrophysics Pioneers Program. The author and other collaborators are also supported in part by the CRESST II Cooperative Agreement (Agreement Number 80GSFC21M0002.